

RAPID COMMUNICATIONS

Rapid Communications are intended for the accelerated publication of important new results and are therefore given priority treatment both in the editorial office and in production. A Rapid Communication in Physical Review B may be no longer than four printed pages and must be accompanied by an abstract. Page proofs are sent to authors.

Lattice distortion of NiO under high pressure

Taizo Sasaki

National Research Institute for Metals, Tsukuba 305, Japan

and JRCAT—National Institute for Advanced Interdisciplinary Research 1-1-4, Higashi, Tsukuba 305, Japan

(Received 22 May 1996)

The lattice distortion under high pressure of an antiferromagnetic material NiO has been investigated within the density-functional formalism with the local-spin-density approximation, using the optimized pseudopotential method and plane-wave basis sets. The result of the calculation shows that the magnetic distortion is enhanced by applying hydrostatic pressure. This distortion becomes extremely large at pressures greater than about 60 GPa. Furthermore, the first-order phase transition from the distorted rocksalt to the cesium-chloride structure is calculated to occur at 318 GPa.

[S0163-1829(96)50338-3]

The structural properties of the transition-metal oxides under high pressure have been investigated extensively motivated mainly by the geophysical interests. The equations of state of some of those materials have been measured up to 20–30 GPa by Clendenen and Drickamer.¹ In their experiment, however, noticeable change in the structure has not been observed except for MnO. Recent studies have revealed several high-pressure phases of FeO such as the rhombohedral phase above near 16 GPa at room temperature² and the NiAs phase at pressures higher than about 80 GPa.³ In contrast to FeO, the high-pressure study on NiO has been limited to relatively low-pressure region and any structural change has not been observed up to about 30 GPa.^{1,4–6}

NiO is known to be an antiferromagnetic material with the Néel temperature of 523 K. Its paramagnetic phase crystallizes in the cubic rocksalt (*B1*) structure. Below the Néel temperature, the magnetic moments are aligned ferromagnetically on the plane perpendicular to the body diagonal direction of the rocksalt cell, and the moments on the adjacent planes are coupled antiferromagnetically to each other. Accordingly, the rocksalt cell is distorted along the direction of the antiferromagnetic ordering, becoming a contracted rhombohedral cell. The rhombohedral angle α_{rh} , which is 60° for the undistorted cell, is measured to be 60.08° at room temperature.⁷

Several theoretical studies on the structural properties

have been done for this material. Yamashita and Asano⁸ applied the local-spin-density approximation (LSDA) of the density functional theory and have shown that the experimental equilibrium lattice constant can be explained within a few percent. Similar results were reported by others.^{9,10} However, these studies have focused on the zero-pressure properties and, to my knowledge, the structural change of NiO due to pressure has not been investigated theoretically.

Considering the fact that most of the *AB*-type ionic compounds in the *B1* structure show a structural phase transition to the cesium-chloride (*B2*) structure, the similar phase transition can be expected for NiO. Theoretically, it can be easily seen that the *B2* structure has a lower electrostatic energy than the *B1* structure, where the electrostatic energy is defined as the static Coulomb energy of the positive ion cores in the compensating uniform negative charge. Thus, as the pressure is applied to decrease the volume, this energy overcomes the band-structure energy and the *B2* structure becomes more stable than the *B1* structure for this kind of compound.

The *B2* structure can be obtained from the *B1* structure by a continuous distortion along the body diagonal direction so that $\alpha_{rh} = 90^\circ$. In the case of NiO, the lattice distortion along the same direction already occurs under ambient condition due to the antiferromagnetic order of spins as mentioned before. Thus, it can be expected that the antiferromagnetic or-

der would somehow affect the structural properties under pressure. This paper reports the results of the theoretical investigation on this issue.

In this study, the total energies of NiO in the distorted *B1* and *B2* phases have been calculated as a function of volume within the density-functional formalism.¹¹ Previous studies have shown that structural properties at normal pressure calculated with the LSDA are in good agreement with the experiment as mentioned before and that the gradient correction does not affect those results significantly.¹⁰ Thus, the exchange-correlation energy was evaluated with the LSDA,¹² using the Ceperley-Alder form.^{13,14}

The Kohn-Sham equations were solved self-consistently in terms of the pseudopotential method. The pseudopotentials were generated with the optimized pseudopotential scheme proposed by Rappe *et al.*¹⁵ with cutoff radii of 0.846 Å and 0.635 Å for Ni and O, respectively. The partial-core-correction scheme¹⁶ was used to include a part of the core charge of the Ni atom in the calculation of exchange-correlation energy since the valence charge density of Ni has a large overlap with the core charge. In this scheme the core charge density was replaced by a smooth function inside a radius of 0.318 Å, which introduces an error of less than 1 mRy/atom in the spin-flip energy of an isolated Ni atom.

The pseudo-wave-functions were expanded with the plane wave basis set of which kinetic energy is less than 70 Ry. The *3d* pseudo-wave-function behaves smoothly in the core region deviating significantly from the all-electron wave function. However, recently, it has been shown¹⁷ that the pseudopotential scheme of the present study can reproduce accurately the all-electron results for ferromagnetic Fe and Ni. In fact, the obtained eigenvalues of the Kohn-Sham equations for NiO agree with those of the previous calculation⁹ with the augmented-spherical-wave (ASW) method within 5 mRy.

The number of *k* points used in the *k*-space integration are 60 and 35 for the distorted *B1* and *B2* structures, respectively, in the irreducible part of the Brillouin zone. The total energy is converged within a few mRy per cell with respect to the cutoff energy and the number of *k* points. The error in the structural parameters is less than a few percent. The stable structure of the distorted *B1* structure is determined by calculating the total energies for various distortions and fitting them to the polynomials.

The results calculated for the ground-state properties, equilibrium lattice constants, bulk modulus, and pressure derivative of the bulk modulus, for the distorted *B1* structure are summarized and compared with experiment in Table I. These values were obtained by fitting the total energies calculated in a volume range of 14.82-18.52 Å³/f.u. to the Murnaghan equation of state.¹⁸ The equilibrium volume is in good agreement with the measured value within 3.4%. Accordingly, error in the calculated lattice constants is less than 2%. Experimentally, the distortion of the *B1* structure contracts the cubic lattice along the body-diagonal direction. The measured rhombohedral angle α_{rh} is 60.08° at room temperature,⁷ and extrapolated to 60.27° at zero temperature.¹⁹ The calculated α_{rh} at normal pressure is 60.53°, indicating that the correct direction of the distortion is obtained.

Figure 1 shows the calculated pressure change of the lat-

TABLE I. The calculated equilibrium volume (V_0), lattice constants (a and c), bulk modulus (B_0), and pressure derivative of the bulk modulus (B'_0) for the distorted *B1* and *B2* structures. The experimental values measured at 22 °C are also listed.

	V_0 (Å ³ /f.u.)	a (Å)	c (Å)	c/a	B_0 (GPa)	B'_0
Distorted <i>B1</i> structure						
Calc.	17.61	2.93	7.10	2.42	236	4.28
Expt. ^a	18.22	2.96	7.23	2.445	184	
B2 structure						
Calc.	16.22				325	3.54

^aReference 7.

tice constants a and c , which are expressed in the hexagonal lattice. It can be seen that both a and c decrease linearly and their compressibilities are close to each other up to about 60 GPa. In the higher-pressure region, the compressibilities become different: The pressure derivative of a becomes positive, while that of c does not show any remarkable change.

To investigate the pressure change of the lattice distortion in detail, we plot the c/a ratio at each pressure in Fig. 2. It can be expected that the lattice distortion from the cubic symmetry decreases by applying pressure, since the itineracy of valence electrons increases at smaller volumes and the magnetic moment, which is the origin of the lattice distortion, is reduced. In contrast to this expectation, Fig. 2 shows that the c/a ratio departs from the value of the undistorted case, meaning that the lattice distortion enhances by pressure. Moreover, corresponding to the stiffness of the a axis in the high-pressure region, c/a shows a significant change at pressures higher than about 60 GPa. The pressure derivatives of c/a in the low- and high-pressure regions are 0.85×10^{-3} and 2.8×10^{-3} GPa⁻¹, respectively.

A similar calculation for FeO has been performed by Isaak *et al.*²⁰ Based on the results for FeO, they suggested that the lattice distortion of NiO decreases under hydrostatic

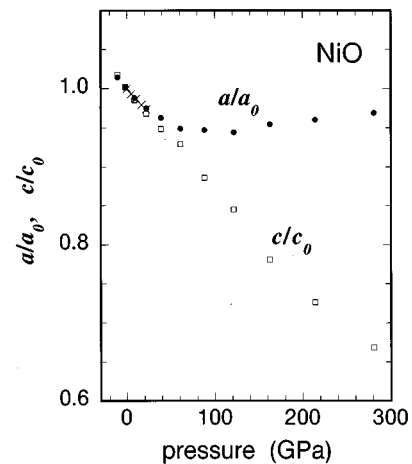


FIG. 1. Pressure dependence of normalized lattice constants a and c , expressed in the hexagonal system, of the distorted *B1* structure. Some experimental values taken from Ref. 6, in which the anisotropic compression is not distinguished, are also plotted by the crosses.

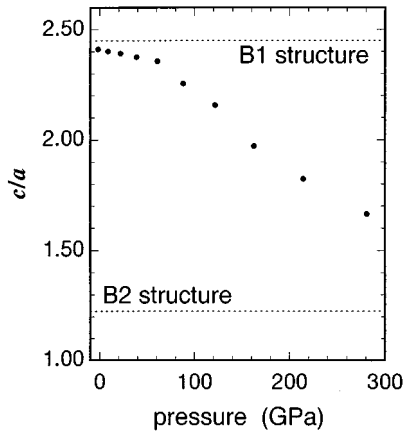


FIG. 2. Pressure dependence of the c/a ratio. The broken lines indicate c/a 's of the undistorted $B1$ ($c/a=6^{1/2}$) and $B2$ $[(3/2)^{1/2}]$ structures.

pressure. However, the present result contradicts their suggestion.

To analyze the rhombohedral distortion of the lattice under pressure, the total energy will be expanded with respect to the shear strain ϵ . From the group-theoretical consideration, it can be shown that this expansion contains the first-order term of ϵ which couples with the antiferromagnetic order. The coefficient of this term becomes zero when there is no antiferromagnetic order. Thus the total energy can be written as

$$E(\epsilon; V) = E_0(V) + a(V)\epsilon + b(V)\epsilon^2 + c(V)\epsilon^3 + d(V)\epsilon^4 + \dots \quad (1)$$

In the present study, the coefficients up to the fourth-order term were determined by fitting the calculated total energies to Eq. (1). The result shows that $b(V)$ changes in its sign at the volume of $13.5 \text{ \AA}^3/\text{f.u.}$ as depicted in Fig. 3 while the volume dependencies of $a(V)$ and $d(V)$ are rather small. The absolute value of $c(V)$ is so small that the third-order term can be neglected in this equation. Thus, the rhombohedral distortion under pressure is governed mainly by the second-order term of ϵ .

$b(V)$ can be divided into two parts: One is the contribution from the electrostatic energy which is defined as the static Coulomb energy of the uniformly distributed valence electrons and the compensating positive point charges (+10 for Ni and +6 for O). The other is the band-structure-energy contribution. Figure 3 also shows the volume dependence of each part. From this figure, it can be seen that the electrostatic-energy contribution has large volume dependence in comparison with the contribution from the band-structure energy. Therefore, it is concluded that the lattice instability of the distorted $B1$ phase under high pressure is driven by the electrostatic energy.

From these analyses, the large change in the lattice distortion can be understood as follows: Near normal pressure the magnitude of the lattice distortion is determined by balancing the magnetic distortion term $a(V)\epsilon$ with the elastic term $b(V)\epsilon^2$. With decrease of the volume, the latter term becomes small in comparison with the former. After the change of the sign of $b(V)$, the elastic term no longer works as the restoring force to the distortion, and finally the large lattice distortion occurs.

The equation of state of the $B2$ phase was determined as in the case of the distorted $B1$ phase. The obtained param-

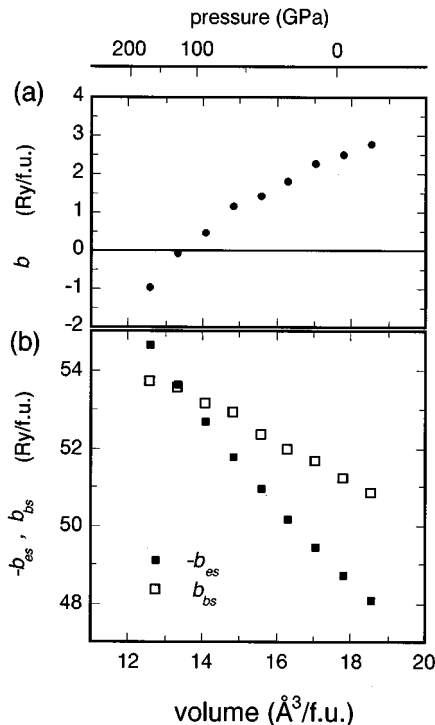


FIG. 3. Volume dependence of the coefficient (a) $b(V)$, and (b) the electrostatic-energy [$b_{es}(V)$] and band-structure-energy [$b_{bs}(V)$] contributions. In (b), both contributions are indicated by close and open squares, respectively.

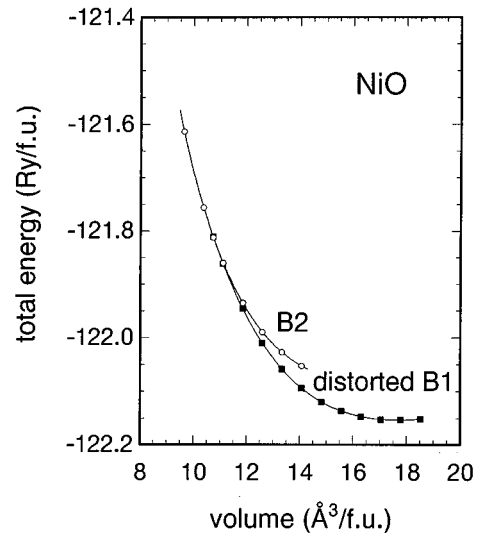


FIG. 4. Total energy of the distorted $B1$ and $B2$ structures of NiO. The points indicate calculated energies and the solid line for the $B2$ structure is a fit to the Murnaghan equation of state. The solid line for the distorted $B1$ structure is the interpolation of the calculated points.

eters are listed in Table I. The total energy of the *B2* phase was calculated by assuming the paramagnetic state. The ferromagnetic configuration and some of the antiferromagnetic ones were examined at $11.11 \text{ \AA}^3/\text{f.u.}$ by starting the self-consistent calculation with the superposition of the atomic spin density which was arranged corresponding to each magnetic state as the initial spin density: In the antiferromagnetic state, the periodicity with a double-size cell was assumed along the $[100]$ or $[111]$ direction. The obtained self-consistent spin distributions did not have any finite value within the accuracy of the calculation. The calculated eigenvalues of the Kohn-Sham equations are found to have finite density of states at the Fermi level, indicating that this phase is metallic.

Figure 4 shows the crystal total energies calculated for the distorted *B1* and *B2* structures of NiO. It can be seen that the distorted *B1* structure is a more stable form than the *B2* structure at normal pressure, which is consistent with experiment. As pressure increases, the distorted *B1* structure undergoes a phase transition into the *B2* phase. Combining the equation of state of the *B2* phase with that of the distorted *B1* phase determined at $10.37\text{--}13.34 \text{ \AA}^3/\text{f.u.}$, the transition pressure is calculated to be $318 \pm 10 \text{ GPa}$. The calculated volume

change is 1.5% of the volume of the lower-pressure phase, $10.97 \text{ \AA}^3/\text{f.u.}$

In this paper, the LSDA of the density-functional theory has been applied to an antiferromagnetic material NiO to study its structural properties under high pressure. The calculation has been performed with the optimized pseudopotential method. The result of the total-energy calculation has shown that the lattice constants and the magnetic distortion at normal pressure are successfully explained. From the calculation at smaller volumes, the following have been predicted: With increasing pressure, the lattice distortion from the cubic symmetry increases in spite of the reduction of the magnetic moment. Furthermore, the pressure dependence of the distortion becomes extremely large above 60 GPa. It was shown that this pressure change of the lattice distortion is driven by the electrostatic energy. Finally the *B2* phase will appear at 318 GPa.

I would like to thank Professor T. Oguchi and Dr. Ohno for fruitful discussions. The present calculations were performed with the JRCAT Supercomputing System and the Numerical Materials Simulator of NRIM.

-
- ¹R. L. Clendenen and H. G. Drickamer, *J. Chem. Phys.* **44**, 4223 (1966).
²T. Yagi, T. Suzuki, and S. Akimoto, *J. Geophys. Res.* **90**, 8784 (1995).
³Y. Fei and H. K. Mao, *Phys. Rev. B* **47**, 266 (1994).
⁴I. Wakabayashi, H. Kobayashi, N. Nagasaki, and S. Minomura, *J. Phys. Soc. Jpn.* **25**, 227 (1968).
⁵J. H. Manghnani, *Trans. EOS.* **73**, 579 (1992).
⁶E. Huang, *High Pres. Res.* **13**, 307 (1995).
⁷C. J. Toussaint, *J. Appl. Crystallogr.* **4**, 293 (1971).
⁸J. Yamashita and S. Asano, *J. Phys. Soc. Jpn.* **52**, 3514 (1983).
⁹K. Terakura, A. R. Williams, T. Oguchi, and J. Kübler, *Phys. Rev. Lett.* **52**, 1830 (1984); K. Terakura, T. Oguchi, A. R. Williams, and J. Kübler, *Phys. Rev. B* **30**, 4734 (1984).
¹⁰T. C. Leung, C. T. Chang, and B. N. Harmon, *Phys. Rev. B* **44**, 2923 (1991).
¹¹P. Hohenberg and W. Kohn, *Phys. Rev.* **136**, B864 (1964).
¹²O. Gunnarson and B. I. Lundqvist, *Phys. Rev. B* **13**, 4274 (1976).
¹³D. M. Ceperley and B. J. Alder, *Phys. Rev. Lett.* **45**, 566 (1980).
¹⁴J. Perdew and A. Zunger, *Phys. Rev. B* **23**, 5048 (1981).
¹⁵A. M. Rappe, K. M. Rabe, E. Kaxiras, and J. D. Joannopoulos, *Phys. Rev. B* **41**, 1227 (1990).
¹⁶S. G. Louie, S. Froyen, and M. L. Cohen, *Phys. Rev. B* **26**, 1738 (1982).
¹⁷T. Sasaki, A. M. Rappe, and S. G. Louie, *Phys. Rev. B* **52**, 12 760 (1995).
¹⁸F. D. Murnaghan, *Proc. Natl. Acad. Sci. USA* **30**, 244 (1944).
¹⁹*Numerical Data and Functional Relationships in Science and Technology*, Landolt-Börnstein, Group III, Vol. 7, Pt. b1 (Springer-Verlag, Berlin, 1975).
²⁰D. G. Isaak, R. E. Cohen, M. J. Mehl, and D. J. Singh, *Phys. Rev. B* **47**, 7720 (1993).